

Reduction of Nitro Aromatic Compounds by Zero-Valent Iron Metal

ABINASH AGRAWAL¹ AND
PAUL G. TRATNYEK*

Department of Environmental Science and Engineering,
Oregon Graduate Institute of Science & Technology,
P.O. Box 91000, Portland, Oregon 97291-1000

The properties of iron metal that make it useful in remediation of chlorinated solvents may also lead to reduction of other groundwater contaminants such as nitro aromatic compounds (NACs). Nitrobenzene is reduced by iron under anaerobic conditions to aniline with nitrosobenzene as an intermediate product. Coupling products such as azobenzene and azoxybenzene were not detected. First-order reduction rates are similar for nitrobenzene and nitrosobenzene, but aniline appearance occurs more slowly (typical pseudo-first-order rate constants 3.5×10^{-2} , 3.4×10^{-2} , and $8.8 \times 10^{-3} \text{ min}^{-1}$, respectively, in the presence of 33 g/L acid-washed, 18–20 mesh Fluka iron turnings). The nitro reduction rate increased linearly with concentration of iron surface area, giving a specific reaction rate constant ($3.9 \pm 0.2 \times 10^{-2} \text{ min}^{-1} \text{ m}^{-2} \text{ L}$). The minimal effects of solution pH or ring substitution on nitro reduction rates, and the linear correlation between nitrobenzene reduction rate constants and the square-root of mixing rate (rpm), suggest that the observed reaction rates were controlled by mass transfer of the NAC to the metal surface. The decrease in reduction rate for nitrobenzene with increased concentration of dissolved carbonate and with extended exposure of the metal to a particular carbonate buffer indicate that the precipitation of siderite on the metal inhibits nitro reduction.

Introduction

Over the last several years, a great deal of interest has developed in the groundwater remediation community over the prospects of new treatment strategies based on dechlorination by granular iron metal. The apparent success of the first field demonstration at Base Borden, Ontario (1), has led to the initiation of numerous feasibility studies, pilot tests, and small to medium scale demonstration projects (2, 3). These developments have created a need for more process-level insight into the chemistry of these systems in order to explain, predict, and/or enhance their performance.

* Corresponding author e-mail address: tratnyek@ese.ogi.edu.

¹ Present address: Department of Geological Sciences, Wright State University, Dayton, OH 45435.

589 28
16-000674

The first detailed studies of halocarbon degradation by iron metal in laboratory batch systems (4, 5) made several fundamental considerations apparent: (i) halocarbon degradation occurs by dechlorination through a surface reaction with the metal as the ultimate electron donor; (ii) the major determinants of degradation kinetics are mass transfer to, area of, and condition of the metal surface; and (iii) mediation by H_2 , metal impurities, or microorganisms do not appear to be necessary for rapid degradation. Concurrent studies performed in laboratory columns (5, 6) showed that halocarbon degradation occurs similarly in porous media, but that there is an important additional consideration: geochemical evolution of the matrix material by iron dissolution and precipitation over the course of extended operation. Many additional studies of contaminant remediation with zero-valent metals have now been reported (2, 7–9). These studies support the view that contaminant degradation results from reduction coupled to metal corrosion, and most address at least one additional factor, such as the range of contaminants that may be remediated with reducing metals, the effect of groundwater geochemistry on remediation performance, or the possibilities for enhanced performance with derivative technologies.

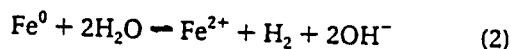
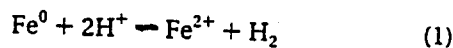
The remediation of nitro aromatic compounds (NACs) is of interest because the nitro aromatic moiety is among the most characteristic of anthropogenic contaminants, being second in this regard only to organochlorine functional groups. NACs are common environmental contaminants because of their use as munitions, insecticides, herbicides, pharmaceuticals, and industrial feed stock chemicals for dyes, plastics, etc. (10). They also may be formed in the environment from aromatic contaminants, as is the case with the nitro-PAHs and nitrophenols found in atmospheric waters (11, 12). Among the processes contributing to the environmental fate of NACs (13), reduction of the nitro group is certainly the most characteristic. The transformation reaction generally produces the corresponding aromatic amines, with minor amounts of intermediates (hydroxylamines and nitroso compounds) and coupling products (azo and azoxy compounds). However, since aromatic amines are still of concern as environmental contaminants, remediation of NACs requires transformation beyond nitro reduction. Two possible means for obtaining complete removal of NAC transformation products are (i) biodegradation, which sometimes occurs more rapidly for aromatic amines than for the parent nitro compounds (14) and (ii) incorporation into natural organic matter by enzyme-catalyzed coupling reactions (15). In principle, either technique could be coupled to nitro reduction with Fe^0 and the combination applied to treat environmental contamination by NACs.

In this study, we investigated the reduction of nitrobenzene by iron metal in bicarbonate-buffered batch systems to (i) assess the potential utility of nitro reduction by Fe^0 in groundwater remediation, (ii) further our understanding of the reactivity of Fe^0 with organic solutes in aqueous systems, and (iii) gain insight into the role that precipitation of solids such as FeCO_3 may play in remediation performance under geochemical conditions. The results indicate that nitro reduction by Fe^0 is significantly faster than

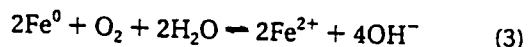
dechlorination (which has already been shown to be effective in field applications) but that the primary products are aromatic amines. Thus, nitro reduction by iron may be of direct use in treatment of waters contaminated with NACs, if the resulting amines can be removed by subsequent treatment. Beyond the direct relevance of nitro reduction to remediation objectives, the reaction was used as a probe technique with which to study the behavior of Fe⁰ in aqueous systems. For this purpose, the advantages of NAC reduction over dechlorination include the following: (i) volatilization of the organic reactant and its reduction products is much less significant, (ii) the specific rate of reaction is more rapid, and (iii) the reaction products do not include chloride, which itself is a strong promoter of corrosion.

Background

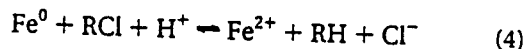
Oxidation of Fe⁰. Zero-valent iron metal, Fe⁰, is readily oxidized to ferrous iron, Fe²⁺, by many substances. In aqueous systems, this phenomenon leads to dissolution of the solid, which is the primary cause of metal corrosion. Metal corrosion is an electrochemical process in which oxidation of Fe⁰ to Fe²⁺ is the *anodic* half-reaction. The associated *cathodic* reaction may vary with the reactivity of available electron acceptors. In anoxic pure aqueous media, the acceptors include H⁺ and H₂O, the reduction of which yields OH⁻ and H₂. Thus, the overall process of corrosion in anaerobic Fe⁰-H₂O systems is classically described by the following reactions:



The preferred cathodic half-reaction under aerobic conditions involves O₂ as the electron acceptor. In this case, the primary reaction yields only OH⁻ and not H₂:



Other strong electron acceptors (oxidants), both inorganic and organic, may offer additional cathodic reactions that contribute to iron corrosion. Systems containing HCO₃⁻ and H₂CO₃ species may act as electron acceptors to oxidize Fe⁰ and promote metal corrosion (16-18). Organic oxidants also react with Fe⁰, as illustrated by the dehalogenation of chlorinated hydrocarbons, RCl:



Reaction 4 can contribute significantly to the net dissolution of iron, even in predominantly aqueous systems (19). NACs also exhibit facile reduction by Fe⁰, but this reaction is not a significant contributor to material damage by corrosion and therefore has not been studied in detail from the corrosion perspective.

Chemical Transformations of NACs. Under reducing conditions, NACs may react by a variety of pathways, which are summarized in Figure 1. Most of these reactions have been studied in great detail either as preparative methods in synthetic chemistry or as model reactions for electrochemical investigations, and numerous reviews on these topics are available (20-23). In almost all cases, the major process is reduction of the nitro functional group to the corresponding amine (Figure 1, reactions I-III). Formally,

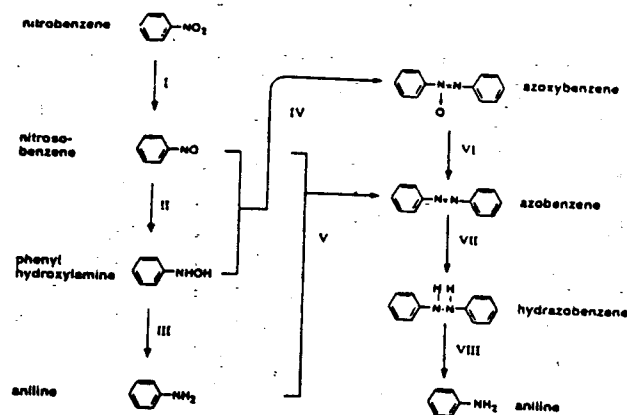


FIGURE 1. Schematic diagram showing the various possible transformation pathways for nitrobenzene in reducing environments. Downward arrows (reactions I-III and VI-VIII) indicate reduction reactions, and right-facing arrows (reactions IV-V) indicate condensations. The dominant reduction pathway of the nitro group to its amino equivalent may occur sequentially via nitroso and hydroxylamine (reactions I-III).

this process consists of a series of two-electron additions, proceeding through nitroso and hydroxylamino intermediates. However, the reduction potentials for reactions I and II are very similar, so polarography performed on acid to neutral aqueous solutions gives only two waves: the first corresponding to a four-electron reduction for formation of the hydroxylamine, and the second corresponding to a two-electron reduction of the hydroxylamine to the amine. At alkaline pH, only one six-electron wave is observed. Accumulation of the nitroso compound is rarely found in practice, and special techniques are often necessary to obtain direct evidence for its formation (24, 25). Indirect evidence for its formation is abundant, however, because condensation reactions involving the nitroso intermediate (reactions IV-V) give azoxy and azo compounds, which are frequently observed in significant yields from nitro reduction (26-28). Product distributions may be further complicated by reduction of the condensation products (reactions VI-VIII) (29) or rearrangements such as the formation of benzidine (not shown) (30).

Reduction of NACs is well documented for aqueous media containing zero-valent metals such as Fe, Zn, or Sn because these reactions have been used widely in the synthesis of amines (31). According to a method that originated with an early study by Lyons and Smith (32), high yields can be obtained using Fe⁰ and trace amounts of salts containing Fe²⁺ or Cl⁻. In addition to the formation of amines, dissolving metal reductions of NACs may produce good yields of the other products represented in Figure 1. For example, reduction of nitrobenzene with Zn is reported to be useful for preparation of phenylhydroxylamine (33). In general, however, yields of products other than amines are usually small and variable, so the reaction is of limited synthetic utility and has received little attention in the recent literature.

In environmental media, reduction of NACs occurs by both biotic and abiotic means (34). The dominant reaction pathway under anaerobic environmental conditions appears to be nitro reduction to the amine. However, there is evidence for most of the other pathways in Figure 1, including coupling of nitro reduction intermediates to form azo and azoxy compounds, and reductive cleavage of azo compounds to form amines (35). The former reaction is of particular importance because azo and azoxy compounds

their precursors. The aromatic amines formed by nitro reduction are subject to additional reactions in environmental systems including covalent binding to natural organic matter (36) or adsorption to mineral surfaces (37). In addition to the reactions included in Figure 1, environmental transformation of NACs can include further degradation by microorganisms. This is likely to include hydroxylation and cleavage of the aromatic ring with eventual mineralization, but such reactions are not expected by the direct action of reducing metals alone.

Experimental Section

Chemicals. Nitro aromatic compounds and their likely reaction products were obtained in high purity from Aldrich and Chem Service and used as received. These included nitrobenzene, 1-chloro-4-nitrobenzene, 1,3-dinitrobenzene, 4-nitrotoluene, 4-nitroanisole, 2,4,6-trinitrotoluene, parathion, nitrosobenzene, aniline, azobenzene, and azoxybenzene. Roughly 1 mM stock solutions were prepared in deionized water (18 M Ω -cm Nanopure) with up to 5% (v/v) HPLC-grade methanol. The bicarbonate buffer media were prepared by flowing deoxygenated 1% CO₂ in N₂ or 100% CO₂ (i.e., pCO₂ = 0.01 and 1.0 atm, respectively) for roughly 2 h through a 15 mM NaOH solution in deionized water. Analytical grade CO₂ and other gases were deoxygenated prior to use by passing through a heated column of reduced copper. The pH range available from the above method was between 5.5 and 8.0, as determined by pCO₂ and the aqueous alkalinity. To prepare more acidic buffers, the initial NaOH solution was modified by the addition of HCl prior to sparging with CO₂.

The iron metal used in this study (Fluka electrolytic iron, catalog no. 44905) was selected to give manageable nitro reduction rates in the experimental system described below. Compared with the Fe⁰ used in our previous studies (4, 6), this material has a coarser grain size (mostly > 40 mesh) and clean, smooth surfaces with a high metallic luster. The nominal purity is 99.9% with the remainder consisting primarily of iron oxide. Trace impurities are less than 0.02% C, 0.008% S, 0.003% Si, 0.002% P, 0.002% Mn, and 5 ppm Mg. The surface area of a 18–20 mesh sieved iron sample prior to acid treatment was determined to be 0.005 m²/g by gas adsorption using BET analysis.

Iron Pretreatment. Prior to use, the Fe⁰ grains were hand-sieved to constrain grain size to 18–20 mesh and sonicated in 10% HCl (v/v) for 20 min to remove surface oxides or other contaminants. The cleaned metal was washed four times with the bicarbonate buffer to remove residual acidity or chloride remaining after the acid treatment. The entire acid-washing procedure was performed under a stream of deoxygenated N₂ with freshly deoxygenated bicarbonate buffer to avoid further surface oxidation to metal oxides. A series of control tests indicated that the mass of Fe⁰ lost due to this pretreatment was 4.9 ± 0.2%. The BET surface area of the iron sample following the acid-treatment increased to 0.038 m²/g.

Model Reaction Systems. Individual degradation experiments were performed in anaerobic (sealed) batch systems prepared in 60-mL serum bottles. In most cases, bottles received 2 g of dry, sieved iron. Following the acid wash, the bottles were filled with fresh bicarbonate buffer medium and crimp-sealed using thick butyl rubber septa (Pierce). Before initiating degradation experiments, each

bottle was allowed 2 h to equilibrate on an end-over-end rotary shaker at 10 rpm in a dark, 15 °C room.

Early experiments in unbuffered Fe–H₂O systems resulted in the expected pH rise (> 2 units in ~4 h) due to aqueous corrosion of the metal (eqs 2 and 3). Although previous batch studies of dechlorination by Fe⁰ have not shown evidence that the pH rise due to aqueous corrosion significantly effects contaminant degradation rates (4), we favored buffered systems for this study to gain greater control over experimental conditions. Previous studies have used various biological buffers in batch systems containing Fe⁰ and not found any specific buffer effects (4, 7, 8). A bicarbonate buffer with total dissolved carbonate = 1.5 × 10⁻² M was adopted for routine experiments because it provided a reasonable buffer capacity without visible precipitation of iron carbonates during the course of a typical degradation experiment (4–5 h).

A typical reduction experiment began by the addition of 1 mL of 10⁻³ M deoxygenated aqueous stock solution of nitrobenzene (or nitrosobenzene, or one of the substituted nitrobenzenes) by needle injection through the septum. Standard incubation conditions were maintained throughout each experiment (i.e., dark, 15 °C, 10 rpm). Loss of parent organic compound and formation of reduction products were determined by periodically removing 200- μ L samples for immediate analysis by HPLC. The BET surface area of the iron sample obtained from serum bottles after the reduction experiment was 0.021 m²/g.

Analyses. The concentrations of unreacted substrate and its various reaction products were determined by isocratic HPLC with UV absorbance detection. The analytical column (4 mm × 10 cm) consisted of Microsorb packing (particle size, 3 μ m) with a C-18 stationary phase. A precolumn (4.6 mm × 1.5 cm) of the same material was also used. The eluent consisted of 60/40 acetonitrile and water (in most cases, buffered with Trizma at pH = 7) with a flow rate of 0.9 mL/min. The absorbance was monitored at 270 nm, which is close to the λ_{max} for nitrobenzene (272 nm) and nitrosobenzene (280, 300 nm). Peaks were identified by comparison with the retention times of standard compounds, and concentrations were determined from peak areas by comparison to standard curves. Surface area was estimated by BET Kr-gas adsorption (Micromeritics) on samples that were prepared by rapidly drying the metal with methanol and storing under N₂ to avoid surface oxidation.

Results and Discussion

Pathway of Nitro Reduction by Fe⁰. The reaction of nitrobenzene by Fe⁰ under the conditions of this study produced aniline with nitrosobenzene as an intermediate product. Accounting for these three species gives good mass balance at pH > 5.5 (> 85%), but with a reproducible dip at intermediate times (Figure 2), which suggests that all of the nitrosobenzene formed is not in solution and/or that there is an additional reaction intermediate. Phenylhydroxylamine is the most likely intermediate and may correspond to an unidentified peak with retention time = 1.2 min (cf. ~1.0 min for the solvent peak, 2.2 min for aniline, 3.7 min for nitrobenzene, and 4.2 min for nitrosobenzene). Similar elution patterns have been reported for nitrobenzene reduction in other systems (24, 38). The variation in size of this peak with reaction time suggests an intermediate in reduction from nitrosobenzene to aniline, and similar behavior was observed when nitrosobenzene was used as

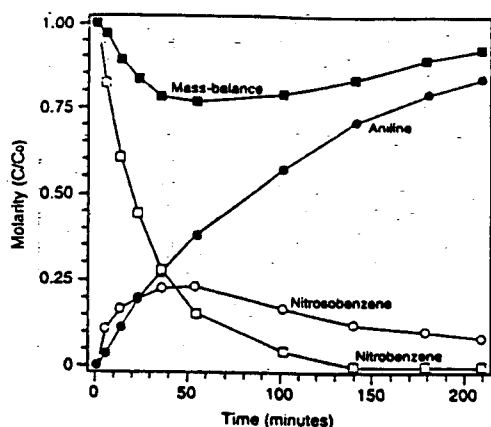


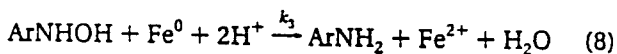
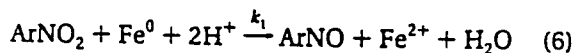
FIGURE 2. Kinetics of nitrobenzene reduction to nitrosobenzene and then to aniline under standard conditions: 33.3 g/L 18–20 mesh acid-washed Fluka iron turnings, pretreated in 1.5×10^{-2} M bicarbonate buffer ($p\text{CO}_2 = 0.01$ atm) for 2 h, mixed throughout by rotation at 10 rpm and 15 °C. Data plotted relative to the initial concentration of nitrobenzene (1.5×10^{-5} M).

the initial substrate. However, a standard for phenylhydroxylamine was not available, so this assignment was not confirmed. Neither azoxybenzene or azobenzene were observed as products of nitrobenzene reduction, indicating that condensation reactions (pathways IV–V, Figure 1) are insignificant at the substrate concentrations used in this study. The absence of detectable azo and azoxy intermediates suggests that reduction of these compounds (i.e., pathways VI–VIII, Figure 1) was not a significant contributor to the formation of aniline.

Based on these results, sequential nitro reduction to aniline via intermediate nitroso and hydroxylamine compounds appears to be the only important transformation process occurring in the $\text{Fe}^0\text{-H}_2\text{O-CO}_2$ systems studied. Formally, the overall reaction



occurs in three steps, each involving a two-electron reduction, with Fe^0 as the ultimate electron donor. The contributing two-electron reactions can be written as



where each k represents the observed first-order rate constant for the associated reduction step. The distribution of products depends on the relative values of these rate constants, which, in turn, will vary with reaction conditions.

Kinetics of Transformation. Experiments were generally performed with nitrobenzene at an initial concentration of about 1.5×10^{-5} M, and the reaction was monitored until >98% complete (~3 h). Loss of nitrobenzene was found to be <5% over 48 h in control experiments without Fe^0 , so all of the disappearance during the first few hours was attributed to nitro reduction. Natural log concentration versus time plots for nitrobenzene reduction were unambiguously linear over at least 3 half-lives (Figure 3), so linear

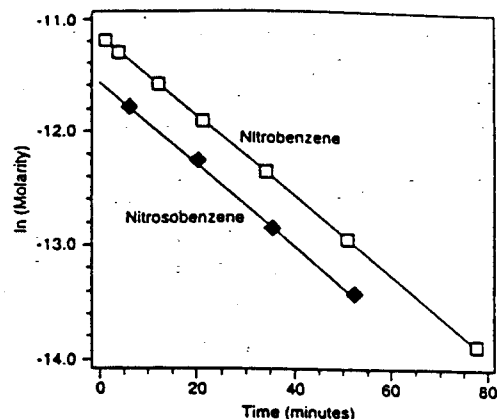


FIGURE 3. Pseudo-first-order disappearance of nitrobenzene (same experiment as Figure 2) and nitrosobenzene (separate experiment under identical conditions). Linear regression gives reduction rate constants of $k_1 = 0.035 \pm 0.001 \text{ min}^{-1}$ ($t_{1/2} = 19.7 \text{ min}$) for nitrobenzene and $k_2 = 0.034 \pm 0.001 \text{ min}^{-1}$ ($t_{1/2} = 20.4 \text{ min}$) for nitrosobenzene.

regression on these data was used for routine determination of k_1 , the pseudo-first-order rate constant for eq 6. The average standard deviation for nitro reduction rate constants determined for several series of replicate experiments was <2.5%. As was concluded previously for the dechlorination of CCl_4 (4), the lack of deviation from first-order kinetics indicates that changes in reactivity of the Fe^0 due to corrosion and precipitation are not significant over several hours. However, nitro reduction experiments that were allowed to run to completion did exhibit a small decline in k_1 at exposure times over 1 h. A similar decline in rates was observed by Gillham and O'Hannesin for the reduction of chlorinated aliphatics in batch experiments (5).

First-order rate constants for the appearance of nitrosobenzene were obtained by nonlinear regression, assuming a kinetic model for sequential first-order reactions is appropriate (4). For the data in Figure 2, the rate constant is $0.069 \pm 0.010 \text{ min}^{-1}$, which is roughly twice the value $k_1 = 0.035 \pm 0.001 \text{ min}^{-1}$ obtained by fitting the data for nitrobenzene disappearance. The discrepancy is modest, but appears to be significant, and suggests an additional reaction for nitrosobenzene formation. One such reaction might be the dismutation of phenylhydroxylamine (39), but no effort was made to test this hypothesis experimentally.

The kinetics of nitrosobenzene reduction (eq 7) were also investigated in two ways. Using nitrosobenzene as the initial substrate, pseudo-first-order disappearance was observed, and therefore k_2 could be obtained simply by linear regression of the natural log concentration versus time data. Alternatively, the concentration of nitrosobenzene as an intermediate in nitrobenzene reduction could be fit by nonlinear regression to the kinetic model for sequential first-order reactions. For similar conditions, the value of k_2 obtained from sequential nitrobenzene reduction ($0.006 \pm 0.001 \text{ min}^{-1}$, Figure 2) was significantly less than that obtained from nitrosobenzene as the initial substrate ($0.034 \pm 0.001 \text{ min}^{-1}$, Figure 3). This difference may be due to competition for reactive sites on the metal by nitrobenzene and its sequential reduction products. The reduction of phenylhydroxylamine (eq 8) was accessible only in terms of aniline appearance. The kinetics of aniline appearance in Figure 2 fit a first-order model with a rate constant, k_3 , of $0.009 \pm 0.001 \text{ min}^{-1}$. The relatively slow rate of aniline appearance is consistent with previous

TABLE 1

Effect of Substitution on Pseudo-First Order Rate Constant of Substrate Reduction^a

substrate ^b	D (cm ² s ⁻¹) ^c	$E_{1/2}$ (V) ^d	k_1 (min ⁻¹)	$t_{1/2}$ (min)
nitrobenzene	6.8×10^{-6}	-0.55 (49)		
nitrosobenzene	7.1×10^{-6}	-0.63 (50)	0.0339	20.4
1,3-dinitrobenzene	6.2×10^{-6}	-0.25 (51)	0.0339	20.4
4-chloronitrobenzene	6.2×10^{-6}	-0.40 (52)	0.0336	20.6
4-nitroanisole	5.9×10^{-6}	-0.55 (51)	0.0327	21.2
4-nitrotoluene	6.2×10^{-6}	-0.46 (52)	0.0335	20.7
2,4,6-trinitrotoluene	5.6×10^{-6}		0.0330	21.0
parathion	4.3×10^{-6}	-0.21 (53)	0.0250	27.7

^a Conditions: 33.3 g/L acid-washed 18–20 mesh Fluka granular iron, 1.5×10^{-2} M carbonate buffer at pH 5.9, 10 rpm, and 15 °C. ^b Initial NAC concentration = 1.5×10^{-5} M. ^c Molecular diffusivity estimated for aqueous solution at 15 °C using the method in ref 54. ^d Polarographic half-wave potentials for aqueous solution at pH 7; references given in parentheses.

reports that aniline inhibits corrosion of steel by adsorbing strongly and covering surface sites (40).

Effect of Substrate Properties. The similarity in disappearance rates for nitrobenzene and nitrosobenzene (Figure 3) suggests a fundamental similarity in the rate controlling processes. However, the diffusion coefficients and reduction potentials for these two compounds are very similar (Table 1), so this result alone cannot be used to determine whether the kinetics are limited by diffusion to/from reactive surface sites or by chemical reaction steps (activation control). Therefore, additional experiments were performed with a series of para-substituted nitrobenzenes selected to exhibit a range of diffusive and electronic properties. The resulting values of k_1 (Table 1) show little if any change in nitro reduction rates over a wide range of redox potentials as long as substrate diffusivities are similar. Parathion is the only compound that exhibits a significantly different value of k_1 , consistent with the lower diffusion coefficient that results from the bulky *p*-(*O,O*-diethyl phosphorothioate) substituent on the nitrophenyl ring.

Effects of the Iron Surface. Since the dechlorination of halocarbons by Fe⁰ involves reaction at the metal surface (4, 5), it was anticipated that the condition and quantity of metal surface area would also influence the kinetics of nitro reduction. Previous work has shown that treatment of the metal with dilute HCl prior to each experiment accelerates dechlorination rates and improves the reproducibility of reaction rate determinations (4). In this study, preliminary experiments showed similar effects for nitrobenzene reduction. The greatest increase in k_1 resulted from the combined action of HCl and sonication, so a protocol based on this treatment was adopted for all subsequent experiments. Aside from the practical advantages of increasing the magnitude and reproducibility of the desired reaction rates, our investigations of pretreatment effects also provide insight into the role of the metal surface in contaminant transformation. The observed effect of acid pretreatment may be due to one or more of the following changes: (i) cleaning of the surface by dissolution of metal and breakdown of the passivating oxide layer; (ii) increasing the metal surface area by etching and pitting through corrosion or by mechanical abrasion during sonication; (iii) increase in the density of highly reactive "sites" consisting of steps, edges, and kinks, following corrosion by acid; and (iv) increased concentrations of adsorbed H⁺ and Cl⁻ that persist after pretreatment with HCl.

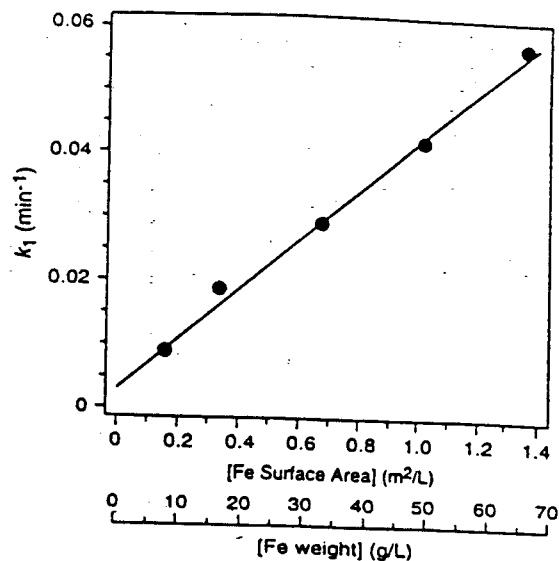


FIGURE 4. Effect of Fe⁰ surface area concentration on the pseudo-first-order rate constant for nitrobenzene reduction. Experiments were performed by varying mass of 18–20 mesh, acid-washed Fluka iron turnings. All were performed in 1.5×10^{-2} M bicarbonate buffer at 10 rpm and 15 °C, after 2 h for buffer equilibration. The regression line corresponds to eq 9.

Under circumstances where the metal surface condition is effectively constant, the quantity of available surface area is among the most significant experimental variables affecting contaminant reduction rates. Figure 4 shows that rate constants for nitrobenzene reduction, k_1 , increase linearly with the mass of Fe⁰ per unit reaction volume (g/L) over the range of conditions studied. Assuming a constant specific surface area of 0.021 m²/g, the more general independent variable of surface area concentration, [surface area], can be derived. Linear regression on the data for k_1 (min⁻¹) and [surface area] (m²/L) gives

$$k_1 = (0.039 \pm 0.002) \times [\text{surface area}] + (0.003 \pm 0.001) \quad (9)$$

with $r^2 = 0.997$ for $n = 5$, and the uncertainties represent one standard deviation. The resulting intercept is statistically significant but negligible under realistic experimental conditions, indicating that other loss processes are minor, and essentially all disappearance is attributable to reaction with Fe⁰. The slope of eq 9 is the specific reaction rate constant; i.e., where k_1 has been normalized to 1 m²/L iron. Reduction rates characterized in these terms should be independent of the mass and specific surface area of the metal used and the volume of the reaction system. At present, however, there is no practical way to factor out variation in the density of reactive sites on the metal surface. The latter correction will be particularly important if meaningful comparisons are to be made between iron samples from different sources or with different histories that affect the type and density of surface precipitates. For example, the 16-fold difference between the values $2.5 \pm 0.2 \times 10^{-3}$ min⁻¹ m⁻² L reported previously for CCl₄ reduction by Fisher Fe⁰ (4) and $3.9 \pm 0.2 \times 10^{-2}$ min⁻¹ m⁻² L determined for nitrobenzene in this study probably reflects, in part, differences in the properties of the two organic reactants. However, reactivity per unit surface area of iron is also likely to be a significant variable because the Fe⁰ source and pretreatment were not the same in the two studies. The specific reaction rate constants described

above other advantages similar to the half-lives normalized to 1 m²/mL that have been reported by Gillham and O'Hannesin (5). One major difference however is that the latter were based on single experiments, so they lack the statistical power that derives from regression on a larger quantity of data, as was done to obtain the fitted parameters in eq 9.

Effect of pH. It was anticipated that changes in pH might cause changes in the nitro reduction rate through (i) direct involvement of H⁺ in the contributing reactions (recall eqs 6–8), (ii) mass transport limitations imposed by the precipitation of a passive film on the metal surface, and/or (iii) mass transport limitations determined by the thickness of the Nernst layer between the passive film and the bulk electrolyte. Previous studies have shown that decreased pH results in a modest increase in CCl₄ dechlorination rate under conditions that probably were borderline between activation and diffusion control (4) and in a strong increase in dechlorination rate where activation control may have been predominant (9). In this study, the results indicate no clear effect on *k*₁ over the environmentally relevant pH range of 6–8 and only a small decrease for pH < 6 (41). The general lack of a pH effect, however, is consistent with nitro reduction rates that are limited by mass transport to reactive sites on a surface where pH-controlled precipitation reactions are comparatively slow (and ionic strength is roughly constant).

A more dramatic effect of pH was observed on the distribution of nitro reduction products. Following the disappearance of nitrobenzene and the intermediate nitroso product, the final concentration of aniline provided nearly complete mass balance at pH > 5. Values of *k*₃, estimated from the rate of aniline appearance, decreased slightly from 0.015 min⁻¹ at pH 5 to 0.009 min⁻¹ at pH 6.9. However, below pH 5, no aniline production at all was detected. It is unlikely that the lack of aniline appearance at pH < 5 indicates a real change in the product distribution since all of the major transformation pathways produce aniline (Figure 1). Instead, protonation of the aniline formed (*pK*_a = 4.6) probably prevents desorption of the product due to electrostatic attractions that involve the anilinium cation and specifically adsorbing counterions such as Cl⁻ (40).

Effect of Mixing Rate. The usual method of mixing employed in this study was 360° rotation at 10 rpm around a fixed-length axis. Since the rate of rotation was rapid relative to the rate of reaction, rpm should be linearly related to the actual velocity of mixing experienced by the metal (at least until centrifugal forces become significant). Numerous empirical determinations have shown that this velocity is proportional to the square of the mass transfer coefficient for diffusion across a stagnant boundary layer (42). Therefore, nitro reduction rate constants should exhibit a linear relationship with respect to (rpm)^{0.5}, under conditions where the reaction is mass transport limited. Values of *k*₁ measured in this study increased linearly with (rpm)^{0.5} up to about 45 rpm (Figure 5), and regression on these data gives

$$k_1 = (0.015 \pm 0.001) \times (\text{rpm})^{0.5} - (0.015 \pm 0.002) \quad (10)$$

where *r*² = 0.998 for *n* = 6. The result provides further evidence for the conclusion that nitro reduction rates are mass transport limited under the conditions of this study.

Effect of Bicarbonate: In most natural waters, ambient levels of pCO₂ and alkalinity determine the pH and

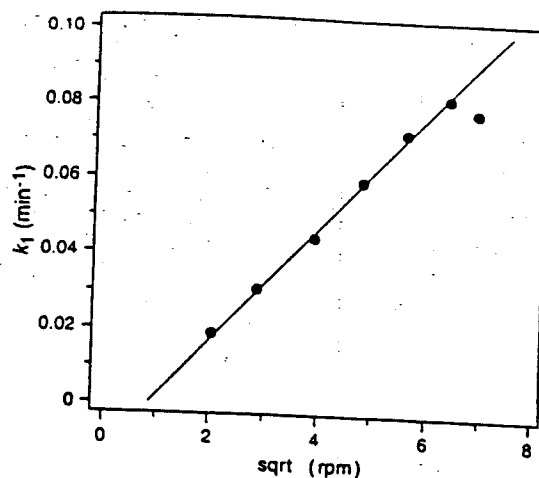


FIGURE 5. Effect of mixing rate on the pseudo-first-order rate constant for nitrobenzene degradation. All bottles contained 33.3 g/L 18–20 mesh acid-washed Fluka iron turnings, pretreated in 1.5×10^{-2} M bicarbonate buffer ($p\text{CO}_2 = 0.01$ atm, initial pH = 7.9) for 2 h, mixed throughout by rotation at 15 °C.

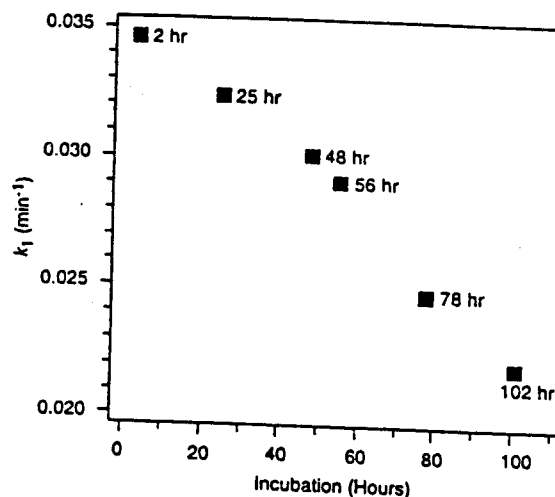


FIGURE 6. Effect of extended incubation of Fluka Fe⁰ with bicarbonate buffer on pseudo-first-order rate constants for nitrobenzene degradation. Bottles containing 33.3 g/L 18–20 mesh acid-washed Fluka iron turnings were pretreated variable amounts of time in 1.5×10^{-2} M bicarbonate buffer ($p\text{CO}_2 = 1.0$ atm, initial pH = 5.9), with mixing throughout by rotation at 10 rpm and 15 °C.

carbonate speciation. In the presence of Fe⁰, H₂CO₃ and HCO₃⁻ can be reduced and thereby accelerate corrosion (17, 18) or precipitate as siderite, which eventually will inhibit corrosion by limiting mass transfer to the metal surface. The net impact of these phenomena on the application of Fe⁰ to remediation of contaminated groundwaters can be predicted from results obtained in this study using CO₂-buffered model systems. In early experiments, it was observed that *k*₁ was notably greater in the presence of moderate concentrations of carbonate buffer relative to unbuffered systems at comparable pH. This increase in *k*₁ appears to be due to carbonate-enhanced corrosion in the absence of significant precipitation. In subsequent experiments, it was discovered that *k*₁ decreased at high total carbonate concentrations [from 0.035 ± 0.001 min⁻¹ at 1.5×10^{-2} M to 0.029 ± 0.001 at 6.0×10^{-2} M (41)] and with extended exposure to a particular bicarbonate buffer (Figure 6). Thus, nitro reduction rates decline as circumstances that favor precipitation of iron carbonates improve. Precipitates such as siderite that are much less redox active than the underlying zero-valent metal generally will inhibit

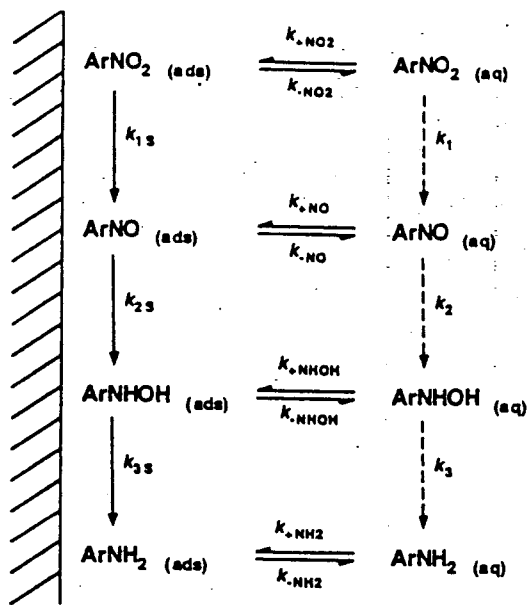


FIGURE 7. Scheme showing competing sequences of substrate adsorption and reduction at a metal surface. The dotted arrows represent the transformation process that was observed by analysis of the solution phase, but reaction took place primarily through adsorption and reduction at the surface (represented by solid arrows).

contaminant reduction by creating a barrier for mass transport to active sites on the metal surface. Therefore, these conditions may prove to be important determinants of field performance in contaminant remediation.

Mechanism of Nitro Reduction. Although mass transport of NACs to the iron surface is rate-limiting and determines the observed first-order rate of disappearance, competition between desorption and further reduction determines the degree to which intermediate transformation products are observed in the solution. This relationship is illustrated in Figure 7 for reduction of nitrobenzene. Appearance of nitrosobenzene as an intermediate in this study implies that its desorption is rapid relative to further reduction to the hydroxylamine (i.e., the step corresponding to k_{-NO} is rapid in comparison to that corresponding to k_{2s}). It is important to note that $ArNHOH_{(ads)}$ must still be formed even though $ArNHOH_{(aq)}$ was not identified, just as $ArNO_{(ads)}$ is believed to be an intermediate in electrochemical nitro reduction even though $ArNO_{(aq)}$ is rarely detected (24, 43). An analogous situation probably exists with dechlorination reactions caused by iron metal. In the latter case, sequential dechlorination is likely to be the dominant reduction pathway at the metal surface (4), even though the distribution of products in solution generally does not show the appropriate amounts of intermediate species. The major reason for this is that the distribution of products observed in the aqueous phase is determined by the rates at which various species undergo desorption and transport away from the metal as well as the intrinsic rates of the reductive dechlorination at the surface.

Aniline cannot be further reduced by iron and, in fact, is a well-known corrosion inhibitor. The mechanism of inhibition is believed to be simple interference with mass transport of oxidant to the metal surface, which in turn is strongly influenced by the orientation of aniline adsorption (40). Corrosion inhibition by this mechanism implies that contaminant reduction rates may also be limited by competition for reactive sites on the metal. This would be

consistent with the kinetics of nitrosobenzene reduction observed in this study (Figures 2 and 3) and may have general significance to the application of Fe^0 as a reducing agent in groundwater remediation.

A likely reduction mechanism for the adsorbed NAC involves the planar donor-acceptor complex as a precursor to electron transfer (23, 44). The adsorbed molecule must undergo a series of electron transfers, proton transfers, and dehydrations to achieve complete reduction, and the order of these steps has been the subject of many detailed electrochemical studies. For example, nitro reduction may be initiated by electron transfer to form an anion radical (43, 45) or by protonation to form a cation which then accepts an electron (46). The precise sequence will vary as a function of pH, solvent properties, and composition of the surface where adsorption and reaction occur. Schwarzenbach *et al.* (38, 47, 48) have concluded that electron transfer is initiating and rate limiting in several homogeneous model systems based on correlations of nitro reduction rates to one-electron reduction potentials. In this study, reduction rates reflect mass transport to the metal surface, so there is no correlation to the energetics of electron transfer. Mass transport also influences the kinetics of further degradation and, therefore, the distribution of detectable reduction products. For this reason, the sequence of electron and proton transfer is unlikely to have a discernible effect on the reaction of NACs by Fe^0 under environmental conditions where the metal surface develops a passivating diffusion boundary of iron oxides or carbonates.

Acknowledgments

The authors acknowledge Mark A. Williamson, Atlantic Geoscience Centre, Geological Survey of Canada for support during manuscript preparation. This study was supported in part by the University Consortium Solvents-In-Groundwater Research Program, the U.S. Environmental Protection Agency through Cooperative Agreement CR 82078-01-0, and the National Science Foundation through Award BCS-9212059. This report has not been subject to review by the U.S. Environmental Protection Agency and therefore does not necessarily reflect the views of the Agency, and no official endorsement should be inferred.

Literature Cited

- O'Hannesin, S. F. M.S. Thesis, University of Waterloo, Ontario, 1993.
- Abstr. Pap.—Am. Chem. Soc.* 1995, No. 209th, pp 689–835.
- Gillham, R. W.; Blowes, D. W.; Ptacek, C. J.; O'Hannesin, S. *Proceedings of the 33rd Hanford Symposium on Health & the Environment—In Situ Remediation: Scientific Basis for Current and Future Technologies*; Battelle Pacific Northwest Laboratories: Columbus, OH, 1994; Vol. 2, pp 913–930.
- Matheson, L. J.; Tratnyek, P. G. *Environ. Sci. Technol.* 1994, 28, 2045–2053.
- Gillham, R. W.; O'Hannesin, S. F. *Ground Water* 1994, 32, 958–967.
- Johnson, T. L.; Tratnyek, P. G. *Proceedings of the 33rd Hanford Symposium on Health & the Environment—In Situ Remediation: Scientific Basis for Current and Future Technologies*; Battelle Pacific Northwest Laboratories: Columbus, OH, 1994; Vol. 2, pp 931–947.
- Schreier, C. G.; Reinhard, M. *Chemosphere* 1994, 29, 1743–1753.
- Lipczynska-Kochany, E.; Harms, S.; Milburn, R.; Sprah, G.; Nadarajah, N. *Chemosphere* 1994, 29, 1477–1489.
- Warren, K. D.; Arnold, R. G.; Bishop, T. L.; Lindholm, L. C.; Betterton, E. A. *J. Hazard. Mater.* 1995, 41, 217–227.
- Hartter, D. R. In *Toxicity of Nitroaromatic Compounds*; Rickert, D. E., Ed.; Hemisphere: Washington, DC, 1985; pp 1–13.

- (11) Kagan, J.; Wang, T. P.; Benight, A. S.; Tuveson, R. W.; Wang, G.-R. *Chemosphere* 1990, 20, 453-466.
- (12) Leuenberger, C.; Czuczwa, J.; Tremp, J.; Giger, W. *Chemosphere* 1988, 17, 511-515.
- (13) Spanggord, R. J.; Mabey, W. R.; Chou, T. W.; Smith, I. H. In *Toxicity of Nitroaromatic Compounds*; Rickert, D. E., Ed.; Hemisphere: Washington, DC, 1985; pp 15-33.
- (14) Dickel, O.; Haug, W.; Knackmuss, H.-J. *Biodegradation* 1993, 4, 187-194.
- (15) Bollag, J.-M. *Environ. Sci. Technol.* 1992, 26, 1876-1881.
- (16) Hardy, L. I. M.S. Thesis, University of Waterloo, Ontario, 1994.
- (17) Wieckowski, A.; Ghali, E.; Szlarczyk, M.; Sobkowski, J. *Electrochim. Acta* 1983, 28, 1619-1626.
- (18) Wieckowski, A.; Ghali, E.; Szlarczyk, M.; Sobkowski, J. *Electrochim. Acta* 1983, 28, 1627-1633.
- (19) Archer, W. L.; Simpson, E. L. *Ind. Eng. Chem. Prod. Res. Dev.* 1977, 16, 158-162.
- (20) Fry, A. J. In *The Chemistry of Amino, Nitroso, and Nitro Compounds and Their Derivatives*; Patai, S., Ed.; Wiley-Interscience: Chichester, 1982; Vol. 1, pp 319-337.
- (21) Zuman, P.; Shah, B. *Chem. Rev.* 1994, 94, 1621-1641.
- (22) Lund, H. In *Organic Electrochemistry*; Baizer, M. M., Ed.; Marcel Dekker: New York, 1973; pp 315-345.
- (23) Holleck, L.; Kastening, B. *Rev. Polarogr.* 1963, 11, 129-140.
- (24) Shindo, H.; Nishihara, C. *J. Electroanal. Chem.* 1989, 263, 415-420.
- (25) Martigny, P.; Simonet, J. *J. Electroanal. Chem.* 1983, 148, 51-60.
- (26) Pizzolatti, M. G.; Yunes, R. A. *J. Chem. Soc. Perkin Trans. 2* 1990, 759-764.
- (27) Dalmagro, J.; Yunes, R. A.; Simionatto, E. L. *J. Phys. Org. Chem.* 1994, 7, 399-402.
- (28) Laviron, E.; Vallat, A. *Electroanal. Chem. Interfacial Electrochem.* 1973, 46, 421-426.
- (29) Gibian, M. J.; Baumstark, A. L. *J. Org. Chem.* 1971, 36, 1389-1393.
- (30) Bunton, C. A.; Rubin, R. J. *Tetrahedron Lett.* 1975, 55-58.
- (31) Hudlický, M. *Reductions in Organic Chemistry*; Ellis Horwood: Chichester, 1984.
- (32) Lyons, R. E.; Smith, L. T. *Chem. Ber.* 1927, 60, 173-182.
- (33) Kamm, O.; Marvel, C. S. In *Organic Syntheses*; Gillman, H., Ed.; Wiley: New York, 1932; Vol. 1, pp 445-447.
- (34) Haderlein, S. B.; Schwarzenbach, R. P. In *Biodegradation of Nitroaromatic Compounds*; Spain, J., Ed.; Plenum: New York, 1995; pp 199-225.
- (35) Weber, E. J.; Wolfe, N. L. *Environ. Toxicol. Chem.* 1987, 6, 911-919.
- (36) Parris, G. E. *Environ. Sci. Technol.* 1989, 19, 1077-1080.
- (37) Haderlein, S. B.; Schwarzenbach, R. P. *Environ. Sci. Technol.* 1993, 27, 316-326.
- (38) Dunnivant, F. M.; Schwarzenbach, R. P.; Macalady, D. L. *Environ. Sci. Technol.* 1992, 26, 2133-2141.
- (39) Wardman, P. *Curr. Top. Radiat. Res. Q.* 1977, 11, 347-398.
- (40) Banerjee, G.; Mallotra, S. N. *Corrosion* 1992, 48, 10-15.
- (41) Agrawal, A. M.S. Thesis, Oregon Graduate Institute, 1995.
- (42) Sherwood, T. K.; Pigford, R. L.; Wilke, C. R. *Mass Transfer*; McGraw Hill: New York, 1975.
- (43) Laviron, E.; Vallat, A.; Meunier-Prest, R. *J. Electroanal. Chem.* 1994, 379, 427-435.
- (44) Kastening, B.; Holleck, L. *Electroanal. Chem. Interfacial Electrochem.* 1979, 27, 355-368.
- (45) Laviron, E.; Meunier-Prest, R.; Lacasse, R. *J. Electroanal. Chem.* 1994, 375, 263-274.
- (46) Zuman, P.; Fijalek, Z.; Dumanovic, D.; Suznjevic, D. *Electroanal. Chem.* 1992, 4, 783-794.
- (47) Heijman, C. G.; Grieder, E.; Holliger, C.; Schwarzenbach, R. P. *Environ. Sci. Technol.* 1995, 29, 775-783.
- (48) Schwarzenbach, R. P.; Stierli, R.; Lanz, K.; Zeyer, J. *Environ. Sci. Technol.* 1990, 24, 1566-1574.
- (49) *Encyclopedia of Electrochemistry of the Elements*; Bard, A. J., Lund, H., Eds.; Marcel Dekker: New York, 1979; Vol. 13.
- (50) Kemula, W.; Krygowski, T. M. In *Encyclopedia of Electrochemistry of the Elements*; Bard, A. J., Lund, H., Eds.; Marcel Dekker: New York, 1979; Vol. 13, pp 131-161.
- (51) Meites, L.; Zuman, P. *CRC Handbook Series in Organic Electrochemistry*; CRC: Cleveland, OH, 1979.
- (52) Kemula, W.; Krygowski, T. M. In *Encyclopedia of Electrochemistry of the Elements*; Bard, A. J., Lund, H., Eds.; Marcel Dekker: New York, 1979; Vol. 13, pp 77-130.
- (53) Smyth, M. R.; Osteryoung, J. G. *Anal. Chim. Acta* 1978, 96, 335-344.
- (54) Tucker, W. A.; Nelken, L. H. In *Handbook of Chemical Property Estimation Methods*; Lyman, W. J., Reehl, W. F., Rosenblatt, D. H., Eds.; McGraw-Hill: New York, 1982; pp 17.1-17.25.

Received for review March 27, 1995. Revised manuscript received July 31, 1995. Accepted August 7, 1995.*

ES950211H

* Abstract published in *Advance ACS Abstracts*, November 1, 1995.